

Research Article

Silvio G. Rotolo*, Maria Luisa Carapezza, Alessandra Correale, Franco Foresta Martin, Gregor Hahn, Alastair G.E. Hodgetts, Mariangela La Monica, Manuela Nazzari, Pierangelo Romano, Leonardo Sagnotti, Gaia Siravo, Fabio Speranza

Obsidians of Pantelleria (Strait of Sicily): A Petrographic, Geochemical and Magnetic Study of Known and New Geological Sources

<https://doi.org/10.1515/opar-2020-0120>

received August 4, 2020; accepted November 5, 2020.

Abstract: This paper provides new petrochemical and paleomagnetic data from obsidian sub-sources on the island of Pantelleria, exploited since the Neolithic. Data has been obtained from 14 obsidian samples from 4 locations: *Fossa della Pernice* (2 sites), *Salto la Vecchia* and *Balata dei Turchi*. Here, we aim to better characterize these obsidians using a cross-disciplinary and multi-analytical approach, to further understand their archaeological significance. Major element analyses (EMP) have enabled two compositional super-groups to be distinguished: (i) *Fossa della Pernice*, less peralkaline and (ii) *Balata dei Turchi–Salto la Vecchia*, distinctly more peralkaline and having almost identical chemical patterns. Trace element analyses (LA-ICP-MS) corroborate major element groupings, with the *Balata dei Turchi–Salto la Vecchia* super-group being further characterized by a pronounced negative europium anomaly. Glass H₂O contents (FT-IR) reveal an overlap among all the sub-sources (H₂O = 0.1–0.3 wt. %). Magnetic methods have refined the petrochemical groupings, permitting further distinction between *Balata dei Turchi–Salto La Vecchia* and the *Fossa della Pernice* super-groups. The occurrence of sub-microscopic (< 1 μm) ferromagnetic minerals results in different magnetic susceptibility and Natural Remanent Magnetization values and allows the best distinction among the products from the chosen sites.

When compared with obsidian tools excavated from Bronze-age settlements on the island of Ustica (230 km NE of Pantelleria), 12% are distinctly peralkaline, indicating their provenance to be from the *Balata dei Turchi* sub-source.

Keywords: Obsidian, Pantelleria, Ustica, Lipari, Bronze age

Article note: This article is a part of Special Issue ‘The Black Gold That Came from the Sea. Advances in the Studies of Obsidian Sources and Artifacts of the Central Mediterranean Area’, edited by Franco Italiano, Franco Foresta Martin & Maria Clara Martinelli.

*Corresponding author: **Silvio G. Rotolo**, Dipartimento di Scienze della Terra e del Mare Università di Palermo (DiSTeM), (Dept. of Earth and Marine Science, University of Palermo), via Archirafi 36, 90123, Palermo, Italy, E-mail: silvio.rotolo@unipa.it

Silvio G. Rotolo, Alessandra Correale, Franco Foresta Martin, Istituto Nazionale di Geofisica e Vulcanologia (National Institute of Geophysics and Volcanology), Sezione Palermo, Italy

Maria Luisa Carapezza, Manuela Nazzari, Istituto Nazionale di Geofisica e Vulcanologia (National Institute of Geophysics and Volcanology), Sezione Roma 1, Italy

Franco Foresta Martin, Laboratorio Museo di Scienze della Terra Isola di Ustica, Italy

Gregor Hahn, School of Geog., Geol. & the Envr., University of Leicester, LE1 7RH, UK

Alastair G.E. Hodgetts, School of Geog., Earth & Envr. Sciences, University of Birmingham, B15 2TT, UK

Mariangela La Monica, Pierangelo Romano, Dept. of Earth and Marine Science, University of Palermo, via Archirafi 36, 90123, Palermo, Italy

Leonardo Sagnotti, Gaia Siravo, Fabio Speranza, Istituto Nazionale di Geofisica e Vulcanologia (National Institute of Geophysics and Volcanology), Sezione Roma 2, Italy

1 Introduction

Throughout the Neolithic, until the Bronze age, obsidian was a widely used geological material across the circum-Mediterranean, primarily used for the manufacturing of stone tools and weapons. Obsidians in the Mediterranean sea occur either as: (i) *peralkaline rhyolites* (i.e. alkali-rich rhyolites) exclusively outcropping on Pantelleria (rare and much less peralkaline obsidians occur also at St. Pietro and St. Antioco islands, Sardinia), or as (ii) *metaluminous rhyolites* (i.e. alkali-poor rhyolites) found at Lipari (Aeolian Islands), Palmarola (Pontine Islands), Mt. Arci (Sardinia), and at Milos, Nisyros, Yali in the eastern Mediterranean. Petrographic and geochemical characteristics have a great efficacy in distinguishing between the above two petrochemical groups, but somehow lose their discriminating power if a given group within the same geological context has different sub-sources.

The distribution of Pantellerian obsidian is quantitatively smaller than that of Lipari but almost equally as widespread. Based on archaeological evidence, movements of this geological material started in the Neolithic, with distribution rapidly declining thereafter (Williams-Thorpe, 1995). The findings of many archaeologists suggest that Pantelleria was not settled before the Ancient Bronze Age (e.g. Tusa, 1997, 2016; Zilhão, 2014), an epoch to which the Mursia Village (the oldest excavated prehistoric settlement on the island) dates back. Mursia is located near to the north-western coast (Figure 1) and has been dated between the 17th and 16th centuries BCE (Tusa, 2016). Traces of Neolithic activity, interpreted as evidence of pre-Bronze Age villages (Leighton, 1999), have also been found on the Pantelleria's north-western side. It is yet to be determined whether the island had permanent settlements since the Neolithic, or if it was merely used as a temporary settlement during seafaring for obsidian trading purposes.

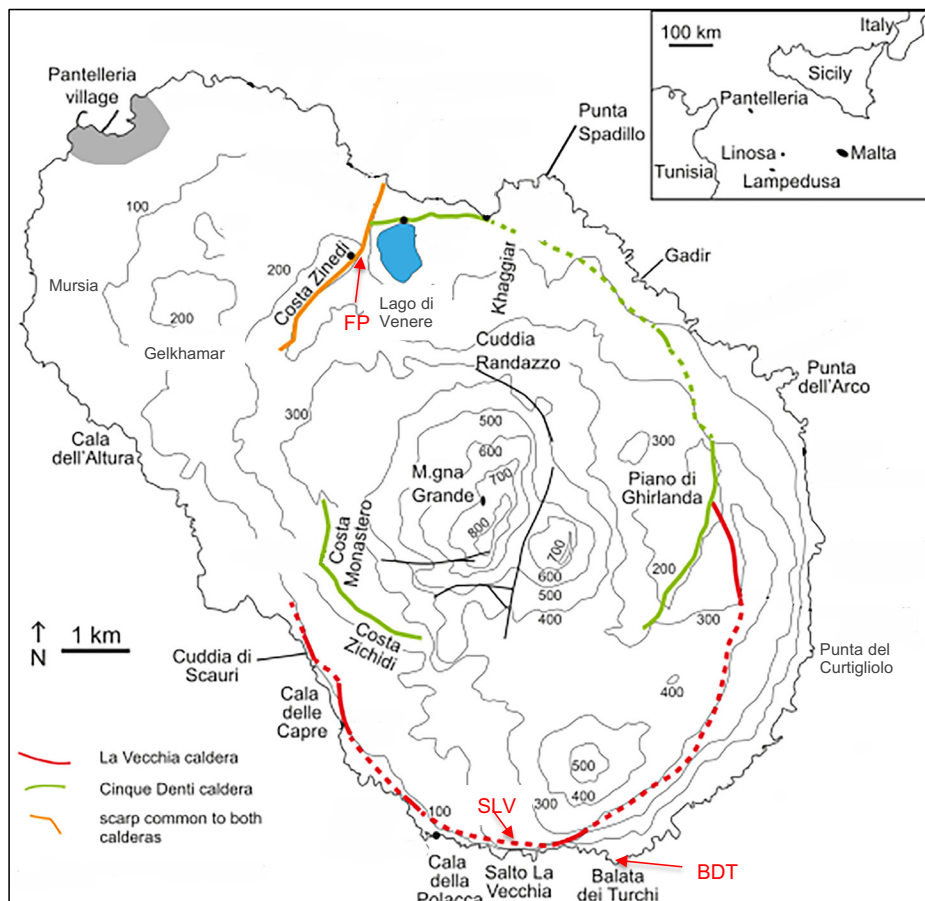


Figure 1: Map of Pantelleria displaying the locations of the four investigated obsidian sites: Fossa della Pernice (FP); Salto La Vecchia (SLV); Balata dei Turchi (BDT). The traces of the two calderas are also shown (modified after Jordan et al., 2018). In the inset the location of Pantelleria within the Strait of Sicily is shown.

The geographical distribution of obsidian artefacts, attributed to Pantellerian quarries, suggests that this island acted as a ‘trading bridge’ between Africa and Europe. Artefacts of confirmed Pantelleria origin have been found in:

- Prehistoric villages in Tunisia (e.g. Kef Hamda, in levels of the 5th millennium BCE); in the island of Lampedusa (Cala Pisana) where obsidian is associated with Stentinellian pottery from the Middle Neolithic (Radi, 1973; Tusa, 2016);
- Malta (Skorba) in levels attributable to the facies of Ghar Dalam and Gray Skorba, dated between the 5th and 4th millennium BCE (Trump, 1966; Tusa, 2016);
- On the relatively small island of Ustica (ca. 70 km north of Palermo, Sicily) at the Spalmatore-Pirozza settlements, where obsidian is associated with Middle Neolithic ceramics (Foresta Martin & Tykot, 2019);
- Milena (Caltanissetta, Sicily) and Roccazzo (Mazara del Vallo, Sicily) where obsidian is found in Eneolithic levels (Tusa, 2016).
- Pescara (Adriatic coast of central Italy) and in southern France (e.g. San Sebastien; Camps, 1974; Crisci, Ricq-de Bouard, Lanzafame, & De Francesco, 1994; Williams-Thorpe, 1995; Tykot, 1996; Mulazzani et al., 2010; Freund, 2014; Freund, Tykot, & Vianello, 2015, 2017).

In order to fully understand the obsidian trade from Pantelleria, the paleogeographic setting must be carefully considered. During the transitional phase in the Mediterranean sea, at the end of the Last Glacial Maximum, navigation between Pantelleria, Africa and Sicily would have been quicker and easier as a result of the lower sea level and consequent exhumation of landmasses from the sea (Leighton, 1999). Pantelleria’s initial ‘fortune’, earned by obsidian trade, could thus be linked to such favourable environmental factors including easy accessibility to the island: sea-level was 15 m lower at 7 ka BP and the Tunisian coast more near (70 km south), relative to the coast of southern Sicily (100 km north) (Abelli et al., 2014).

Furthermore, this island of Ustica, situated almost half-way between Lipari and Pantelleria has been barycentric for trade routes to Sardinia and southern Italy. Recent studies on the archaeometric characterization and provenance of over a thousand obsidian artifacts, collected from settlements on the island spanning the Neolithic and Bronze Age, show an average of 12% imported from Pantelleria, with the majority derived from the island of Lipari (Foresta Martin et al., 2017; Foresta Martin & La Monica, 2019; Tykot & Foresta Martin, 2020).

Pantelleria obsidians occur as small (few m² to some tens of m²), generally < 200 m away from the source vent, rhyolitic lava flows (SiO₂ = 68–75 wt. %) or at the margins (the most rapidly cooled) of crystal-bearing rhyolite flows. Early workers assumed a single extraction site, named Balata dei Turchi, for Pantelleria obsidian (Belluomini & Taddeucci, 1971; Bigazzi, Bonadonna, Belluomini, & Malpieri, 1971), but subsequent studies proposed three to five possible sub-sources around the island (Francaviglia, 1988; Acquafredda, Andriani, Lorenzoni, & Zanettin, 1999; Vargo, 2003; Tykot, 2017a,b; Tufano, D’Amora, Trifuoggi, & Tusa, 2012). Despite the broadly similar pantelleritic composition, some subtle differences in major, trace elements and petrography occur.

This paper aims to:

- (i) Outline the systematic approach used to determine the most appropriate analytical method (e.g. EMP, LA-ICP-MS, FT-IR, and paleomagnetism) to discriminate between similar sub-sources within the same geological context.
- (ii) Obtain an exhaustive petrochemical and petrophysical characterization of exploited obsidian sites on Pantelleria, reviewing the existing literature and adding more robust databases to field and lab characteristics (precise location, macro and microscopic characterization, etc).
- (iii) Compare and correlate the Pantellerian sub-sources with pantelleritic archaeological obsidian tools and weapons discovered in Bronze Age settlements at Ustica, ca. 230 km NNE of Pantelleria.

Furthermore, the paper aims to identify the obsidian sources favoured by ancient miners and traders, to establish the petrochemical and palaeomagnetic differences between obsidian sub-sources and to better understand the role of Pantelleria in the context of established trade ways with the Sicilian mainland and/or the possible geographic influence of the major obsidian producer of ancient times, i.e. the island of Lipari in the Aeolian Archipelago (ca. 330 km NE of Pantelleria).

Finally, at Pantelleria, the misidentification of numerous concentrations of obsidian as indicative of a geological deposit, rather than the remains of intense lithic reduction activity, is highlighted and explored.

2 Pantellerian Archaeological Background

The timing of the human occupation of Pantelleria is considered a significant archaeological puzzle. Studying obsidians from Pantelleria allows further insight into this area of research.

The first and sporadic human presence in Pantelleria seems to have developed before the first stable settlement, due to the abundance of high-quality obsidian that attracted the interest of explorers from both the Sicilian and African mainlands. This hypothesis is based on the fact that the only sizeable prehistoric settlement discovered in Pantelleria, the fortified village of Mursia, has been dated to the period between the Early and Middle Bronze Age. There is solid evidence, albeit indirect, that obsidian from Pantelleria was distributed in various prehistoric villages of the Central Mediterranean as early as the Neolithic (Nicoletti, 1997; Cattani et al., 1997; Tusa, 2016).

All discoveries of Pantellerian obsidians in the western Mediterranean have led archaeologists to hypothesize a flourishing obsidian trade from Pantelleria to other distant villages of the Central Mediterranean during the Neolithic. This was initiated by “rangers” defined by Tusa (2016), i.e. non-resident visitors coming from the mainlands closest to the island, who established activities of exploitation of obsidian outcrops and processing of the raw material on site.

In the territory of Pantelleria this pre-residential activity, chronologically preceding the Bronze Age, would be demonstrated by the existence of “*lithic workshops*” from which it is possible to recover processed products of obsidian and flint.

Dating is problematic, being entrusted only to typological analyses (Cattani et al., 1997; Nicoletti, 2012). A typical example of a lithic workshop is represented by the Punta Fram site, ca. 2 km south of the fortified village of Mursia, which was already reported by the first archaeological studies of the past two centuries (Orsi, 1899; Tozzi, 1968). This “aceramic” lithic industry presents, at the same time, characteristics common to the obsidian works between the Mesolithic and the Neolithic of other Mediterranean settlements, but also similarities with the lithic typologies of the Bronze Age found in the nearby Village of Mursia (Nicoletti, 2012; Tusa, 2016). Therefore, its dating remains unconvincing.

3 Geological Outline of Pantelleria

Pantelleria is the type locality of pantellerite, a peralkaline rhyolite ($\text{SiO}_2 = 68\text{--}72$ wt. %) rich in Na_2O , K_2O , FeO and poor in Al_2O_3 (by definition, the peralkaline composition is when the *peralkalinity index*, **P.I.**, i.e. the molar $\text{Na}_2\text{O} + \text{K}_2\text{O} / \text{Al}_2\text{O}_3$, is > 1.0). Rocks of pantelleritic composition dominate at Pantelleria (others include trachytes and subordinated basalts). Pantellerite magmas have been emitted in three different ways: (i) *lava flows*, producing glassy pantellerite lavas with a variable abundance of alkali feldspar phenocrysts; (ii) *pumice falls*, produced by Strombolian to Plinian eruptions, (iii) *ignimbrites* (rocks produced by the emplacement of pyroclastic density currents).

The eruptive history of Pantelleria is complex, consisting of multiple eruptions with diverse eruptive processes (see Jordan et al., 2018). The volcanism onset occurred ca. 375 ka (Mahood & Hildreth, 1986). Nine eruptions occurred thereafter, with the emplacement of radial pyroclastic density currents with runouts across the entire island (Jordan et al., 2018). The latest large magnitude eruption at Pantelleria is the Green Tuff ignimbrite (sub-Plinian to Plinian) dated at 45.7 ± 1.0 ka (Scaillet, Vita-Scaillet, & Rotolo, 2013) responsible for the Cinque Denti caldera collapse. This ignimbrite appears to ‘drape’ and erode the underlying units, making it distinctively recognisable around the island. The destructive ignimbrite-forming eruptions alternated also with less explosive Strombolian activity and associated lava flows. The most recent on-land eruption is dated at 6-8 ka (Speranza, Landi, D’ Aiello Caracciolo, & Pignatelli, 2010; Scaillet, Rotolo, La Felice, & Vita, 2011).

Obsidians at Pantelleria occur as small, generally < 100 m, rhyolitic lava flows ($\text{SiO}_2 = 68\text{--}75$ wt. %) or are present at the margins (the most rapidly cooled) of crystal-bearing rhyolite flows. In this scenario, crystal-free obsidians are extremely rare, while crystal-bearing *obsidianaceous* rocks, hardly workable, are much more common. *Obsidianaceous* layers occur in Pantelleria as:

- (i) Thin (5–10 cm) glass-rich layers with rare crystals which occur at the base of some ignimbrite sheets (*vitrophyres*);
- (ii) Lava-like glass-rich agglutinates (with rare crystals) produced from compaction of fountain-fed fallout deposits;
- (iii) Sparse lithic clasts in pyroclastic deposits;
- (iv) Crystal-free *hyalo-pantellerite* lavas (very rare: the great majority of pantellerite lavas have feldspar phenocrysts $> 10\%$).

4 Some Consequences of Chemical Differences Between Peralkaline and Metaluminous Rhyolites

Obsidian is phenocryst-free, but generally microlite-bearing (phenocrysts > 500 μm in length, microlites if < 50 μm). It is a vitreous (glassy) volcanic product produced by the rapid cooling of a silica-rich melt, highly viscous so that crystal nucleation and growth is inhibited. Glass is an amorphous solid, lacking the periodic long-range order typical of the crystalline state, which forms for rapid cooling of a generally viscous silicate melt; the higher the magma viscosity, directly related to the SiO_2 content, the more difficult the crystal growth.

Although all rhyolitic magmas are characterized by a high SiO_2 content, (68–75 wt. %), a major distinction separates (i) *peralkaline rhyolites*, higher in Na, K (and Fe), and lower in Al, with respect to (ii) *metaluminous/peraluminous rhyolites*, lower in alkali and higher in Al. These chemical differences can influence the petrographic and physical properties of the rocks, e.g. the liquidus temperature (ie. temperature of the onset of crystallization upon the cooling of a melt) that can be set at ~ 950 °C (at $P_{\text{H}_2\text{O}} = 1$ kbar) for metaluminous rhyolites, opposed to the ~ 780 °C liquidus temperature for peralkaline rhyolites (at $P_{\text{H}_2\text{O}} = 1$ kbar). A strong influence is also on magma viscosity, which is two-three orders of magnitude lower for peralkaline rhyolites at the same temperature (T), pressure (P) and dissolved $\text{H}_2\text{O}_{\text{melt}}$ (Di Genova et al., 2013), due to the role of alkalis in interrupting melt polymerization.

Consequences of the (relatively) low-viscosity of pantellerite magmas include the glass transition temperature (T_g), defined as the temperature (below the T of complete crystallization) that separates a liquid-like (viscous) to solid-like (brittle) rheological response to the applied stress. Peralkaline rhyolites have a lower T_g (around 550 °C for an H_2O -free system, Di Genova et al., 2013) if compared to that of metaluminous rhyolites and this implies that, upon cooling, a pantellerite crystal-free melt has a wider temperature-time window to deform in ductile mode (*rheomorphism*) and to develop folded structures, a pattern directly related to fragility and thus of primary importance for the workability of a glassy rock.

5 Sampling Strategy and Sample Description

5.1 Previous Studies on Pantelleria Obsidian Sources

Previous studies on obsidian sources at Pantelleria call attention to the two most evident and known ones (Balata dei Turchi and Salto La Vecchia), as well as to some other uncertain sources. The latter either lacks an accurate identification of the primary outcrop, or are of poor quality (e.g. crystal-bearing, small clast size, etc.) and/or of difficult access. After a careful screening of literature data and based on our own field surveys, we discarded some of the reported potential obsidian sub-sources for the reasons reported hereafter.

Gelkhamar (Figure 1) (Francaviglia, 1988): it consists of a crystal-bearing hyalopantellerite lava flow, with no known primary obsidian outcrops. It is very likely only a possible workshop site in the archaeological area of Mursia, where Francaviglia (1988) recovered some obsidian clasts.

Lago di Venere: this site was invoked by several authors (e.g. Francaviglia, 1988; Vargo, 2003; Tykot, Freund, & Vianello, 2013) but with no possibility to better locate the obsidian outcrop in a rather vast area. One possibility is that 'Lago' refers to the Fossa Pernice outcrop (selected for this work, see below), which lies on the scar above the lake, ca. 800 m from the northwest edge of the lake and at 180 m elevation. Another possibility referred by Tufano, D'Amora, Trifuoggi and Tusa (2012), is the presence of a thin crystal-bearing obsidianaceous layer at ~ 15 m height above the west shoreline of the lake. This level likely corresponds to the basal vitrophyre (crystal-bearing) of the Green Tuff ignimbrite, which in a few places on the west sector of the lake, plunges towards much older rocks and offers a poor quality obsidian with insufficient exposure to be defined as a possible extraction site. A third, and even less probable site, is at Zinedi (Figure 2A). The Zinedi Formation is an unwelded ignimbrite first described by Jordan et al. (2018). It is located ca. 400 m from the western limit of the lake, at a level ~ 70 m higher, and is best reported by Vargo (2003, her Figure 27), who located and described in detail the obsidian outcrops of Pantelleria. Our work suggests it is highly

unlikely that Zinedi was a usable primary source, given the small dimensions (and rarity) of obsidian lithic clasts and their consequent poor workability.

We therefore hypothesize that clasts recovered in the area of Lago di Venere, as reported by Francaviglia (1984, 1988) are likely wastes of a reduction site dedicated to the first shaping of obsidian blocks before shipping.

Southern coastal sites: other sites on the southern coastal cliffs reported by Tufano et al. (2012) and Rapisarda (2007); *Cala delle Pietre Nere* (below Cuddia di Scauri, Figure 1), *Cala della Polacca*, and *Punta del Curtigliolo* are difficult to access by foot (e.g. exposed on vertical scars at a height of ca. 30–40 m asl). Nevertheless, obsidian clasts fallen from these outcrops are scattered along the shoreline. Their stratigraphic position, within a white tephra fall deposit, places the deposits as older than the Polacca Formation. (Jordan et al., 2018). Although there is no evident continuity of exposure the deposits are likely the same, as from Punta della Polacca to Balata dei Turchi the same agglutinate layer crops out that mantles the paleotopography at various heights (see Figure 3A). Unfortunately, it is not possible to reliably assess whether the much higher (280 m asl) Salto La Vecchia site (due to the almost identical major and trace elements patterns with Balata dei Turchi) also belongs to the same eruptive unit, given the difficulty to trace a continuity east and west of Salto La Vecchia from the coast. Some of the obsidianaceous layers reported by Rapisarda (2007) from Balata dei Turchi to Punta del Curtigliolo, are thin (< 10–15 cm) basal vitrophyres of ignimbrite sheets, hardly workable because they are fractured and crystal-bearing.

5.2 Sampling Sites and Stratigraphic Constraints

We focused on the following four outcrops of primary obsidians (all pantelleritic in composition) individuated after our surveys (Figure 1): (i) *Fossa Pernice 1 (FP 1)*; (ii) *Fossa Pernice 2 (FP 2)*, less than 200 m apart from Fossa Pernice; (iii) *Salto La Vecchia (SLV)*; (iv) *Balata Dei Turchi (BDT)*.

Fission track ages (Bigazzi et al., 1971) date Balata dei Turchi obsidian in an age interval 127–141 \pm 17 ka; this age is consistently underestimated in the light of recent $^{40}\text{Ar}/^{39}\text{Ar}$ ages obtained from older and younger eruptive units (Jordan et al., 2018), which bracket the ages of all these obsidians in the interval 190–240 ka.

All outcrops were assessed before sampling for macroscopic homogeneity (constancy of crystal abundance, absence of colour bands or heterogenous vesicle distribution, etc.) and number of samples taken from each outcrop was proportional to the outcrop length. The compositional homogeneity was later confirmed under the microscope and, more importantly, by the very low standard deviations of several microprobe analyses of different samples from the same outcrop (Tables 2 and 3).

Fossa delle Pernice 1 (FP 1) is a very small (5x2 m) pantellerite lava outcrop, not easily accessible, exposed in the upper section of the Zinedi caldera wall (Figure 2A), at a height of ~170 m asl. The lava is up to 2 m thick and lies conformably above a well-sorted, pumice lapilli fall deposit (Figure 2B). Obsidian is massive, minorly fractured and contains feldspar phenocrysts (5–8 vol. %).

Fossa delle Pernice 2 (FP 2) is a small (10 x3 m) pantellerite lava outcrop positioned ca. 200 m northeast of FP 1, 15 meters below the crest of the Zinedi caldera wall. The basal layer (< 1 m thick) of this unit consists of blue to black partly-fractured obsidian, slightly less crystalline than FP 1 (Figure 2 C).

Salto La Vecchia site (SLV) is an outcrop which can be accessed only from above, (Figures. 3A, 3B, 4A), located at a height of ~280 m on the vertical scar of the La Vecchia caldera wall. It consists of an amygdaloid body of crystal-free pantelleritic obsidian, fractured at the cm scale, around 20 m long with a variable thickness of 1 to 3 m; at places it alternates with centimetric less welded scoriaceous levels.

Balata dei Turchi outcrop (BDT) is exposed at a height variable from 30 to 60 m asl, with access via a debris-fan derived from the erosion of the above cliff (Figures 3A, 3C). It extends laterally for more than 200 m, with a thickness of 0.5–3 m; its source vent is unidentified. The obsidian layer lies conformably on a poorly sorted pumice lapilli which is capped by a 20 cm tuff (Figure 4B). This pantellerite obsidian is almost phenocryst-free and although partly fractured at the cm scale, it contains 10–15 cm unfractured parts and thus represents, together with the obsidian from Salto La Vecchia, the most workable Pantelleria material.

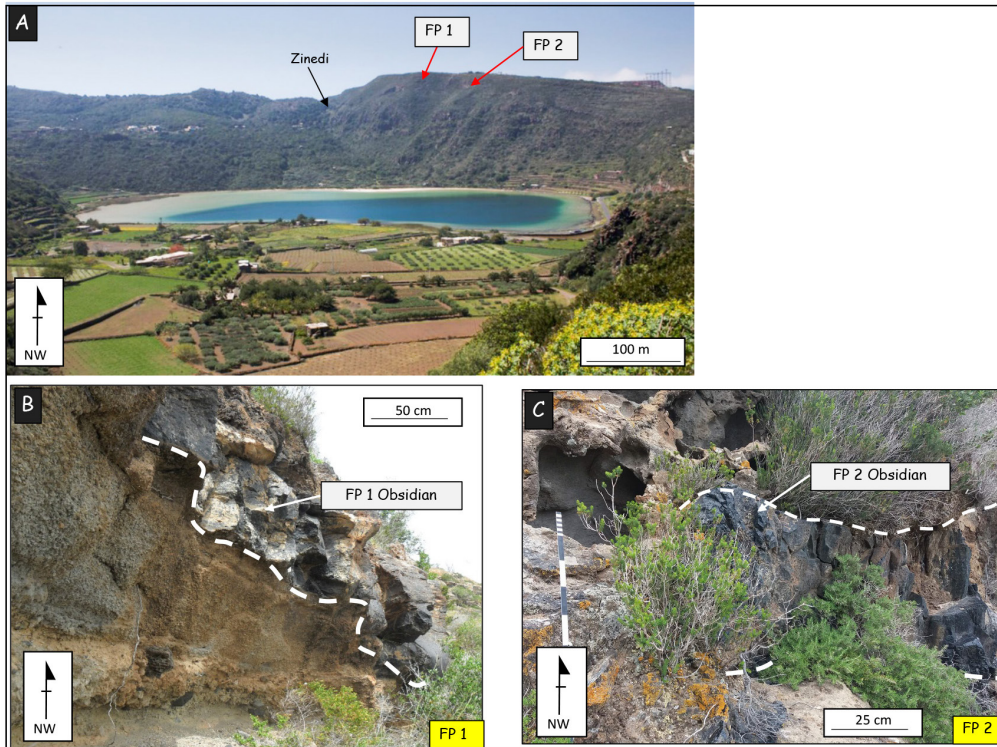


Figure 2: Field photographs showing the two Fossa della Pernice sites (FP 1, FP 2) located in the scarp above Lago di Venere (*Venus' Lake*).

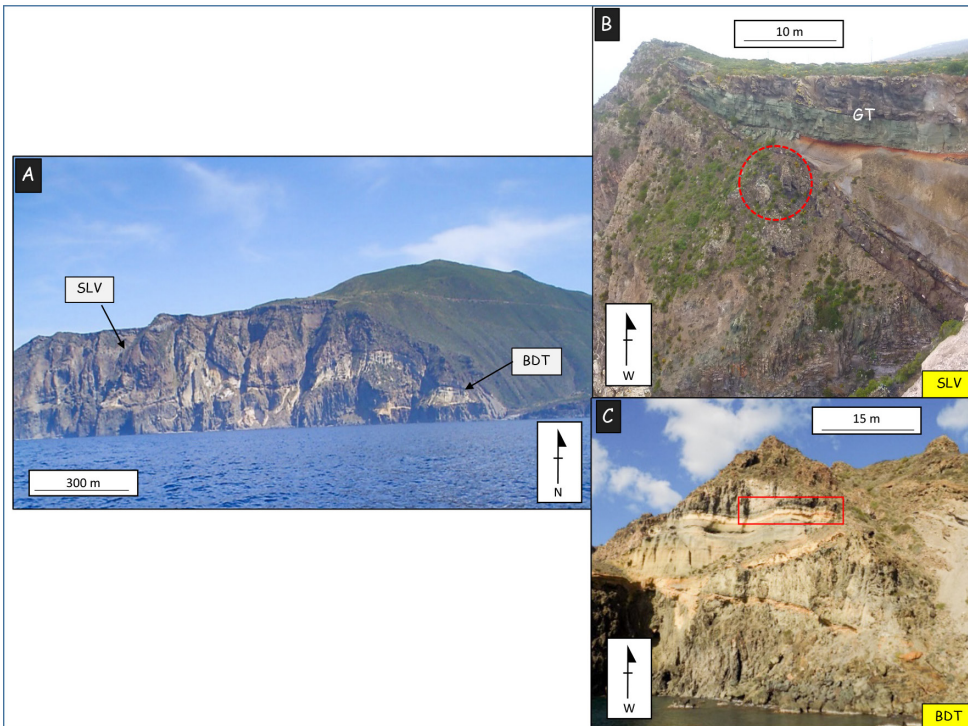


Figure 3: (A) The southern sites of Salto la Vecchia (SLV) and Balata dei Turchi (BDT) in a wide angle and mid-distance view. (B) mid-distance view of the Salto La Vecchia obsidian outcrop, below which there is a 280 m vertical scar, GT = Green Tuff ignimbrite; (C) mid-distance view of the Balata dei Turchi site.

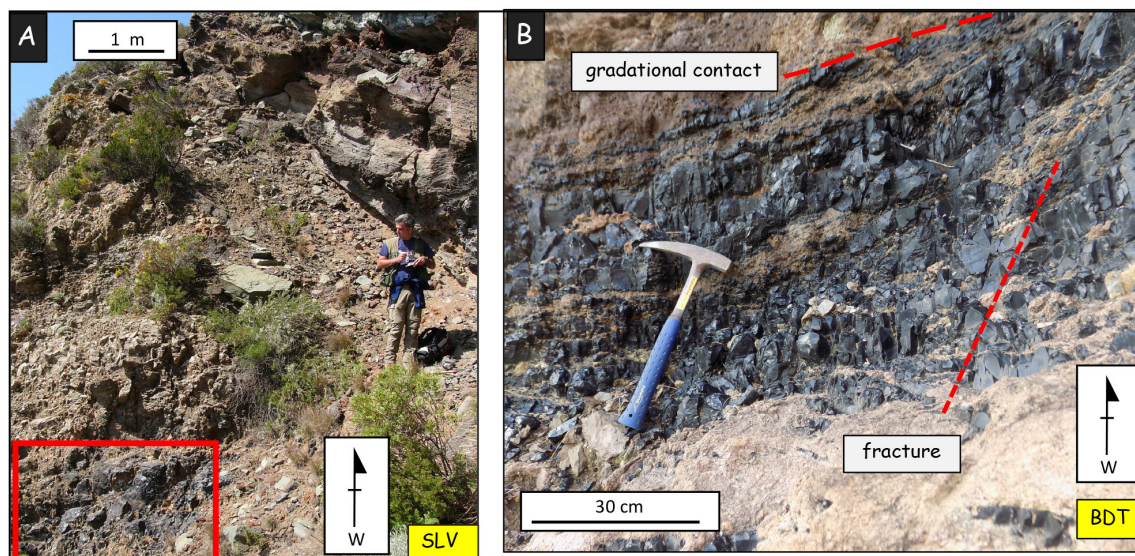


Figure 4: Field photographs displaying the obsidian outcrops. (A) Salto La Vecchia (obsidian in the red area); (B) Balata dei Turchi.

5.3 Sample Description: Petrography

All samples are black with greenish nuances if observed in transparency as thin slices, an attribute exclusive to Pantelleria obsidians. Table 1 displays the principal characteristics of all samples (Figure 5 A, D) which are summarized below:

- **FP 1** samples (Figure 5A) are slightly richer in feldspar phenocrysts, relative to the other Pantelleria samples. In thin section, sparse radiating microlites, a result of incipient glass alteration (devitrification) are noted (Figure 6A).
- **FP 2** samples (Figure 5B) display sparse feldspar phenocrysts (ca. 5 mm in length) and aenigmatite microlites (100–200 μm in length and < 5 vol. %).
- **SLV** samples (Figure 5C) display feldspar microlites arranged in a fluidal manner. These samples are characterized by amphibole microlites (100–150 μm in length, < 5 vol. %, Figure 6B).
- **BDT** samples (Figure 6C) have very rare amphibole and aenigmatite microlites (< 50 μm in length, < 3 vol. %).

6 Analytical Techniques

6.1 Electron Microprobe (EMPA)

Fragments of obsidian glasses (typically 2–5 mm in diameter) were mounted in epoxy resin. Major elements of FP1, SLV and BDT samples were analysed by a JEOL JXA-8200 wavelength-dispersive electron microprobe at the INGV laboratory in Rome. Data were gathered by 5 spectrometers with the instrument conditions set to an accelerating voltage of 15 kV, beam current of 8 nA and a 10 micron defocused beam. Counting times of 5 s for the background and 10 s for the peak were used. The following standards have been adopted for the various chemical elements: albite (Si, Al and Na), forsterite (Mg), augite (Fe), rutile (Ti), orthoclase (K), apatite (F, P and Ca), sodalite (Cl), celestine (S) and rhodonite (Mn). Sodium and potassium were analyzed first to mitigate the effects of alkali migration. The precision of the microprobe was estimated through the analysis of well-characterized synthetic oxides and mineral secondary standards. Based on counting statistics, analytical uncertainties relative to the reported concentrations indicate that precision was better than 5% for all elements.

Major element analyses of FP 2 samples (Z01 and Z02) were carried out using a JEOL JXA-8200 wavelength-dispersive electron microprobe at the Research Laboratory for Archaeology and History of Art, University of Oxford. These glass analyses used an accelerating voltage of 15 kV, beam current of 6 nA and 10 micron beam diameter. Elemental peaks were counted for 12 s for Na, 50 s for Mg, Mn, P, Cl and 30 s for Si, Ca, K, Al, Ti and Fe. Prior to analysis, the

Table 1: Sample localities and principal petrographic features. Fossa della Pernice (FP); Salto La Vecchia (SLV); Balata dei Turchi (BDT). Feldspar (fsp), Amphibole (am); Clinopyroxene (cpx); Aenigmatite (aenig). ⁽¹⁾ Phenocrysts (> 0.5 mm) ⁽²⁾ Microlites (< 50 microns).

| Sample ID | Site | Latitude/longitude | Height (m asl) | Phenocrysts abundance (vol %) ⁽¹⁾ | Phenocrysts (fsp) max lenght (mm) | Microlite ⁽²⁾ types |
|-----------|------|---------------------------------|----------------|--|-----------------------------------|--------------------------------|
| FP1050B | FP 1 | 36°48'53.9" N; 11°58'48.9" E | 175 | 5–8 | 3 | fsp |
| FP1701 | FP 1 | 36°48'53.9" N; 11°58'48.9" E | 175 | 5–8 | 2 | fsp |
| FP1708 | FP 1 | 36°48'53.9" N; 11°58'48.9" E | 171 | 5–8 | 2 | fsp |
| Z01 | FP 2 | 36°49'0.5" N; 11°58'53.9" E | 135 | 3–5 | 2 | fsp, am |
| Z02 | FP 2 | 36°49'0.6" N; 11°58'54.0" E | 135 | 5–8 | 5 | fsp, am |
| SLV 0653 | SLV | 36°44'14.5" N; 12°00'27.8" E | 205 | 1–2 | 1 | fsp, am, cpx |
| BDT 1601 | BDT | 36°44'11.1" N; 12°01'16.6" E | 27 | 1–2 | 2 | fsp, am, cpx, aenig |
| BDT 1602 | BDT | 36°44'10.6"N; 12°01'16.6"E | 34 | 2–3 | 3 | fsp, am, cpx, aenig |
| BDT 1603 | BDT | 36°44'10.7"N; 12°01'16.6"E | 40 | 1 | 1 | fsp, am, cpx |
| BDT 1604 | BDT | 36°44'10.7"N; 12°01'16.5"E | 64 | 1 | 2 | fsp, am, cpx |
| BDT 1605 | BDT | 36°44'09.7"N; 12°01'17.5"E | 55 | 1–2 | 2 | fsp, am, cpx |
| BDT 1606 | BDT | 36°44'10.7"N; 12°01'17.5"E | 47 | 1–2 | 2 | fsp, am, cpx |
| BDT 1607 | BDT | 36°44'10.7"N; 12°01'17.4"E | 49 | 1 | 1 | fsp, aenig |
| BDT 1608 | BDT | 36°44'10.7"N; 12°01'17.4"E | 56 | 1 | 1 | fsp, am, cpx, aenig |
| BDT 1609 | BDT | 36°44'10.7"N; 12°01'17.4"E | 62 | 1 | 2 | fsp, cpx |

electron microprobe was calibrated for each element using primary mineral standards. The accuracy and precision of the calibration was evaluated using secondary standard analyses at the beginning, throughout and at the end of the sample run. Secondary standards used were MPI-DING reference glasses from the Max Plank Institute (Jochum et al., 2006), with analyses lying within the standard deviation of the preferred values. All glass data was normalized to 100% for comparative purposes and to account for variety in hydration, and data were rejected where low analytical totals occurred (< 92 wt. %) or where non-glass analyses (e.g. microlites) had occurred.

6.2 Laser Ablation Inductively Coupled Plasma Mass Spectrometry (LA-ICP-MS)

Trace element compositions of the same sample mounts used before for EMP were investigated at the Istituto Nazionale di Geofisica e Vulcanologia (INGV-Palermo) laboratory using a GeoLasPro 193nm ArF excimer laser ablation (LA) system, connected to an Agilent 7500ce quadrupole ICP-MS. The analyses were performed with a laser repetition rate



Figure 5: Hand-specimen photographs of representative obsidian samples: (A) Fossa Pernice 1; (B) Fossa Pernice 2 (note the feldspar phenocrysts); (C) Salto La Vecchia; (D) Balata dei Turchi.

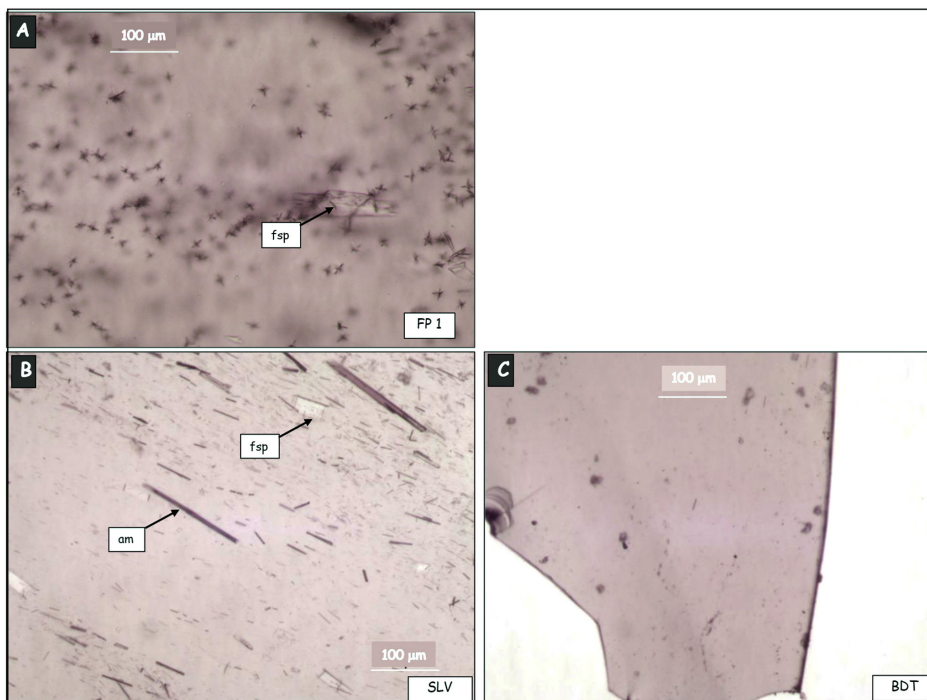


Figure 6: Plane-polarized light microscope photos of obsidian thin sections (magnification 40 X). (A) Fossa Pernice 1: feldspar microphenocrysts and clots of unidentified quench microlites; (B) Salto La Vecchia amphibole and feldspar microlites; (C) Balata dei Turchi: very rare amphibole and aenigmatite microlites poorly visible in the lower half of the photo.

of 10 Hz, a fluency of 15 J/cm², a He flux of 0.8 L/min in the ablation cell. Each obsidian sample was analyzed three times with a 32 micron spot.

Glass reference material NIST612 and ²⁹Si were used as external and internal standard, respectively. The analytical accuracy, calculated by repeated analyses of the USGS basaltic reference glass BCR-2G, resulted to be ≤ 10% for most of the elements whereas the analytical precision (RSD%), estimated by repeated analyses of the reference material NIST612, was ≤ 5% for most of the elements.

6.3 FT-IR Spectroscopy

FT-IR was conducted to determine the water content in obsidian chips. These analyses were carried out at the University of Palermo (DiSTeM) using a Bruker Hyperion 2000 FT-IR spectrometer, coupled with a microscope (fluxed with CO₂- and H₂O-free compressed air). Plane parallel doubly polished obsidian wafers (60–100 μm thick) were mounted on a ZnSe disk for FT-IR analyses. Sample spectra and background were acquired in the 1000–6000 cm⁻¹ absorption range with a resolution of 2 cm⁻¹, adopting a Globar source with a MCT detector and scan rate of 20 kHz and completing 256 scans.

Water concentrations were derived from total H₂O absorption band (3550 cm⁻¹) using a straight baseline correction and applying the Beer-Lambert equation, $c = (MW A)/(d \rho \epsilon)$, where c is the wt. % of dissolved H₂O, MW the molecular weight of H₂O, A the height of the absorption peak, d the sample thickness in cm, ρ the glass density in g L⁻¹, ϵ the molar extinction coefficient. The glass density and molar extinction coefficients calculated as in Lanzo, Landi & Rotolo (2013).

6.4 Rock Magnetic Methods

Rock magnetic measurements were conducted in the shielded room of the Palaeomagnetic Laboratory of the Istituto Nazionale di Geofisica e Vulcanologia (INGV-Rome). The Natural Remanent Magnetization (NRM) of all samples was measured by a 2G Enterprises DC-SQUID cryogenic magnetometer. For each sample, we also calculated the Q Königsberger ratio (e.g. Kono, 2015), i.e. the ratio between remanent (NRM) and induced magnetization intensity. The latter is the product of k (bulk volume susceptibility measured on each sample with a MFK1-Multifunction Kappabridge) and B (the Earth's magnetic field total intensity at Pantelleria, 44,700 nT in 2020 according to the IGRF model).

7 Results

7.1 Major Elements Geochemistry

When *major element* analyses (Table 2) are plotted in the FeO_{tot} vs. Al₂O₃ diagram (Macdonald, 1974) two groups can be clearly distinguished, displaying different clusters (Figure 7):

- Obsidian samples from FP 1 and FP 2 sites are almost identical in their major element contents and are remarkably higher in Al₂O₃ and lower in FeO, i.e. are less peralkaline (P.I. = 1.4–1.5), with respect to the SLV-BDT super-group (P.I. = 2.2).
- Samples belonging to SLV-BDT groups are indistinguishable among themselves, but, if compared with FP samples, are distinctly more peralkaline.

7.2 Trace Elements Geochemistry

Trace elements are coherent with the typical patterns of pantellerites: very high contents of incompatible elements (in particular Zr, Nb, La, Ce) and depleted in Sr, and corroborate the major element analyses. More specifically:

Table 2: Mean and std. deviation (2-σ) of electron microprobe analyses of obsidians. X = n° of analyses for the calculation of the mean. P.I. = Peralkalinity index, molar (Na₂O+K₂O)/Al₂O₃. Site abbreviations as in Table 1.

| Site | FP 1 | | FP 2 | | SLV | | BDT | |
|--------------------------------|--------|----------|--------|----------|--------|----------|--------|----------|
| X= | 16 | st. dev. | 56 | st. dev. | 16 | st. dev. | 16 | st. dev. |
| SiO ₂ (wt%) | 70.47 | 0.21 | 70.26 | 0.12 | 71.68 | 0.27 | 72.22 | 0.31 |
| TiO ₂ | 0.50 | 0.07 | 0.53 | 0.04 | 0.21 | 0.04 | 0.21 | 0.01 |
| Al ₂ O ₃ | 10.61 | 0.09 | 11.12 | 0.07 | 7.48 | 0.12 | 7.51 | 0.16 |
| FeO _{TOT} | 5.73 | 0.10 | 5.91 | 0.07 | 7.63 | 0.13 | 7.13 | 0.49 |
| MnO | 0.29 | 0.04 | 0.29 | 0.02 | 0.32 | 0.05 | 0.29 | 0.02 |
| MgO | 0.21 | 0.02 | 0.20 | 0.02 | 0.03 | 0.02 | 0.03 | 0.00 |
| CaO | 0.36 | 0.04 | 0.38 | 0.02 | 0.24 | 0.03 | 0.25 | 0.02 |
| Na ₂ O | 6.32 | 0.10 | 6.31 | 0.09 | 7.28 | 0.12 | 7.25 | 0.18 |
| K ₂ O | 4.86 | 0.11 | 4.64 | 0.05 | 4.31 | 0.08 | 4.27 | 0.10 |
| P ₂ O ₅ | 0.05 | 0.04 | 0.02 | 0.02 | 0.03 | 0.04 | 0.03 | 0.01 |
| Cl | 0.36 | 0.01 | 0.37 | 0.02 | 0.51 | 0.02 | 0.50 | 0.01 |
| F | 0.23 | 0.06 | n.a. | | 0.28 | 0.05 | 0.31 | 0.05 |
| Total | 100.00 | | 100.00 | | 100.00 | | 100.00 | |
| P.I. | 1.48 | 0.03 | 1.38 | 0.02 | 2.23 | 0.03 | 2.21 | 0.05 |

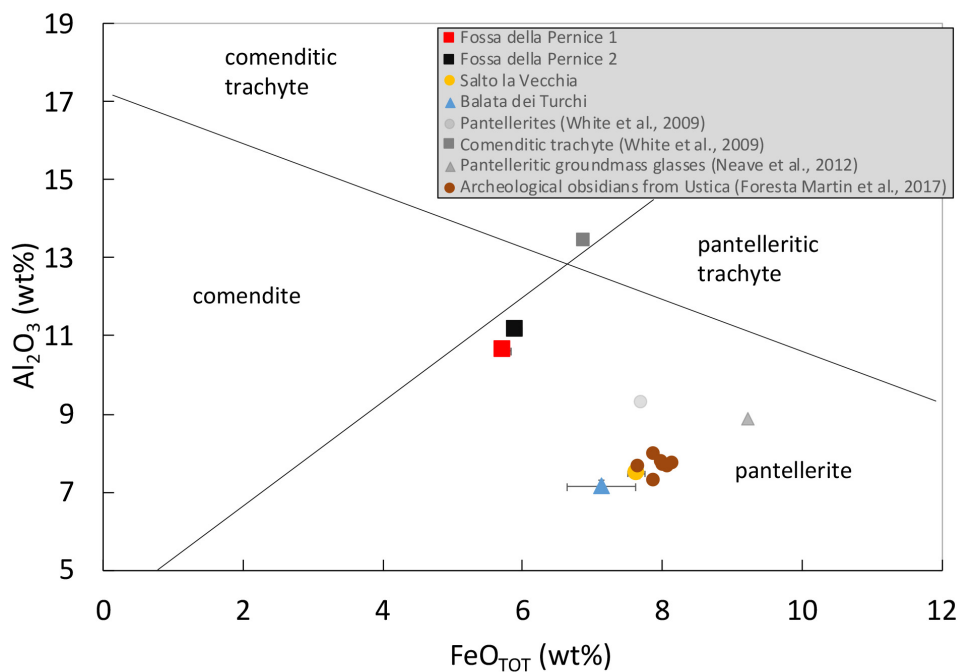


Figure 7: Macdonald (1974) classification diagram for Pantelleria peralkaline rocks (new analyses by electron microprobe). Literature data are whole-rock analyses from White et al. (2009) and electron microprobe groundmass glass analyses from Neave et al. (2012). Selected archaeological obsidians from Bronze age settlements on Ustica with a pantelleritic chemical fingerprint are plotted for comparison (source: Foresta Martin et al., 2017).

- Fossa della Pernice 1 and 2 sites (FP 1 and FP 2) are very similar to each other, except for zirconium, niobium, and hafnium, slightly lower in FP 1 samples (Figure 8A, Table 3).
- The comparison of the three super-groups show the less peralkaline FP samples have lower concentrations in Rb, La, Ce, Nb and Hf but are slightly higher in Ba (Figure 8B, Table 3). FP 1 is also higher in Zr. BDT samples are almost similar to SLV samples; the very small enrichment of SLV samples in incompatible trace elements (Nb, Zr, La, Ce) is just above the 2-sigma standard deviation.

The Rare Earth Elements (REE) distribution in the chondrite-normalized plot (Figure 9) shows a high REE content (e.g. 220 times the chondritic value) with a rather ‘flat’ distribution among light (La, Ce) and heavy REE (Yb, Lu), $Ce_N/Yb_N = 6.8-7.5$ (the subscript _N stands for ‘normalized’ concentration of the given element in the sample to the correspondent concentration in the reference chondrite). Most importantly, although all samples show a strong negative Eu anomaly, this is higher in FP samples with an $Eu_N/Eu^* = 0.35$, in comparison to BDT + SLV with $Eu_N/Eu^* = 0.48$. (Eu^* is the interpolated value between Sm and Gd, i.e. the REE adjacent to Eu in the classical REE plot as in Figure 9; $Eu_N/Eu^* = 1$ means no Eu anomaly, while $Eu_N/Eu^* < 0.5$ means a rather strong negative Eu anomaly). This ratio has a great importance in igneous petrology because, given the strong partitioning of Eu in plagioclase, a negative Eu anomaly indicates a plagioclase fractionation experienced by the magma in its earlier evolution-cooling stages, i.e. is a distinctive and specific magma character.

As a whole, trace elements highlight again that there is a clear discrimination between FP and the BDT-SLV groups, but not within BDT-SLV samples, which are in total overlap.

7.3 The H₂O Content in Obsidian Glass

The H₂O content in the glass may be used to discriminate between similar obsidians, given that post-eruptive hydration is chiefly a function of hydration processes, and hence of the time elapsed since cooling (Stevenson & Novak, 2011); although influenced by a number of secondary variables, such as the degree of glass devitrification/alteration, fracturing/micro fracturing, proximity to the exposed surface, etc.

Our analyses of representative samples did not detect any relevant difference among the three groups, with results (not shown) that are within the error of the method: FP 1: H₂O = 0.20 wt. %; SLV: H₂O = 0.09 wt. %; BDT: H₂O = 0.17 wt. %).

7.4 Rock Magnetic Data

We collected 10 obsidian samples of 1–5 cm³ volume from each site, spread across the outcrops. Natural Remanent Magnetization and magnetic susceptibility data provide valuable information regarding the discrimination of sampling sites (Figure 10A). The four sites (FP 1, FP 2, BDT, SLV) are well discriminated with regards to the NRM values, especially the Balata dei Turchi – Salto LaVecchia sites. Although the Fossa Pernice 2 sub-site (FP 2) yields values more scattered than in other sites, it is still distinguishable due to its high susceptibility values that peak at maximum (2×10^{-3} SI) among the whole data set.

8 Discussion

During the late Neolithic to Bronze age (i.e. 6th to 2nd millennium BCE), two principal obsidian localities were present in the south-western Mediterranean Sea: Lipari and Pantelleria. Obsidian sources on Lipari were closer to the North Sicilian coast, and therefore more accessible as ancient quarries. During this time one of the most exploited (in a later age) Lipari obsidian source, Rocche Rosse, was yet to erupt (eruption age 1200 CE, Martinelli, Tykot, & Vianello, 2019; Tykot, 2019 and references therein). Additionally, between 10 and 5 ka BP, sea level was between 45 and 5 m lower than

Table 3: Mean and std. deviation (2-sigma) of trace element analyses of obsidians obtained by LA-ICP-MS. $X = n^{\circ}$ of analyses for the calculation of the mean. The subscript $_N$ stands for 'normalised' (concentration of the given element in the sample divided by the correspondent concentration in the reference chondrite, chondrite values from McDonough and Sun (1995). $Eu_N/Eu^* < 1$ represents a negative europium anomaly, see text. Site abbreviations as in Table 1.

| Site | FP 1 | | FP 2 | | SLV | | BDT | |
|-------------|---------|-----------------|---------|-----------------|---------|-----------------|---------|-----------------|
| | 12 | <i>st. dev.</i> | 13 | <i>st. dev.</i> | 3 | <i>st. dev.</i> | | <i>st. dev.</i> |
| K (ppm) | 40361.4 | | 44957.3 | 641.9 | 35795.1 | | 35397.6 | 712.5 |
| Ti | 2793.6 | 159.0 | 2219.1 | 44.5 | 2854.3 | 559.9 | 1373.1 | 5.8 |
| Rb | 134.9 | 6.5 | 145.6 | 2.9 | 175.8 | 2.8 | 179.7 | 9.3 |
| Sr | 1.5 | 0.1 | 1.7 | 0.1 | 3.3 | 0.1 | 3.4 | 0.2 |
| Ba | 47.7 | 2.3 | 52 | 1.5 | 20.6 | 0.4 | 20.3 | 1.1 |
| La | 145.6 | 5.7 | 162.15 | 5.0 | 202.3 | 2.4 | 204.6 | 14.6 |
| Ce | 307.3 | 26.2 | 327.3 | 17.5 | 403.9 | 6.3 | 409.6 | 19.2 |
| Pr | 29.6 | 1.4 | 32.7 | 1.0 | 42.3 | 0.3 | 43.5 | 2.6 |
| Nd | 105.4 | 5.8 | 116.8 | 3.9 | 153.7 | 2.4 | 157.5 | 11.3 |
| Sm | 20.1 | 0.8 | 22.5 | 0.8 | 30.3 | 0.7 | 30.3 | 2.4 |
| Eu | 3.1 | 0.2 | 3.5 | 0.1 | 3.4 | 0.0 | 3.5 | 0.3 |
| Gd | 18.7 | 1.4 | 23.9 | 0.6 | 28.9 | 0.5 | 29.7 | 2.9 |
| Tb | 2.9 | 0.2 | 3.5 | 0.1 | 4.3 | 0.1 | 4.4 | 0.4 |
| Dy | 19.0 | 0.9 | 22.4 | 0.7 | 28.0 | 0.1 | 28.5 | 2.4 |
| Ho | 3.7 | 0.2 | 4.5 | 0.1 | 5.4 | 0.1 | 5.4 | 0.5 |
| Er | 10.7 | 0.5 | 12.9 | 0.5 | 15.1 | 0.3 | 15.0 | 1.2 |
| Tm | 1.6 | 0.1 | 1.9 | 0.1 | 2.2 | 0.1 | 2.2 | 0.2 |
| Yb | 10.8 | 0.5 | 12.8 | 0.3 | 14.6 | 0.3 | 14.4 | 1.5 |
| Lu | 1.5 | 0.1 | 1.9 | 0.1 | 2.0 | 0.1 | 2.0 | 0.2 |
| Y | 98.5 | 4.5 | 121.7 | 3.8 | 144.8 | 2.1 | 144.8 | 12.4 |
| Zr | 1336.3 | 62.1 | 1584.8 | 36.9 | 1545.7 | 27.6 | 1575.5 | 127.8 |
| Nb | 267.84 | 12.9 | 286.8 | 14.9 | 331.3 | 4.9 | 341.7 | 12.0 |
| Hf | 26.0 | 1.5 | 32.1 | 0.65 | 34.0 | 0.1 | 33.8 | 3.3 |
| Ta | 15.4 | 0.7 | 17.05 | 0.4 | 20.1 | 0.2 | 20.4 | 1.0 |
| Th | 22.8 | 1.1 | 25.95 | 0.5 | 30.0 | 0.6 | 29.4 | 2.2 |
| U | 7.5 | 0.4 | 7.9 | 0.1 | 9.7 | 0.2 | 9.7 | 0.4 |
| Zr/Y | 13.45 | 0.70 | 13.02 | 0.18 | 10.66 | 0.10 | 10.88 | 0.19 |
| Rb/Sr | 89.90 | 3.62 | 87.54 | 3.13 | 53.27 | 2.62 | 52.83 | 0.43 |
| Eu_N/Eu^* | 0.49 | 0.02 | 0.46 | 0.01 | 0.35 | 0.02 | 0.35 | 0.02 |
| Ce_N/Yb_N | 7.41 | 0.6 | 6.82 | 0.30 | 7.27 | 0.30 | 7.47 | 0.50 |

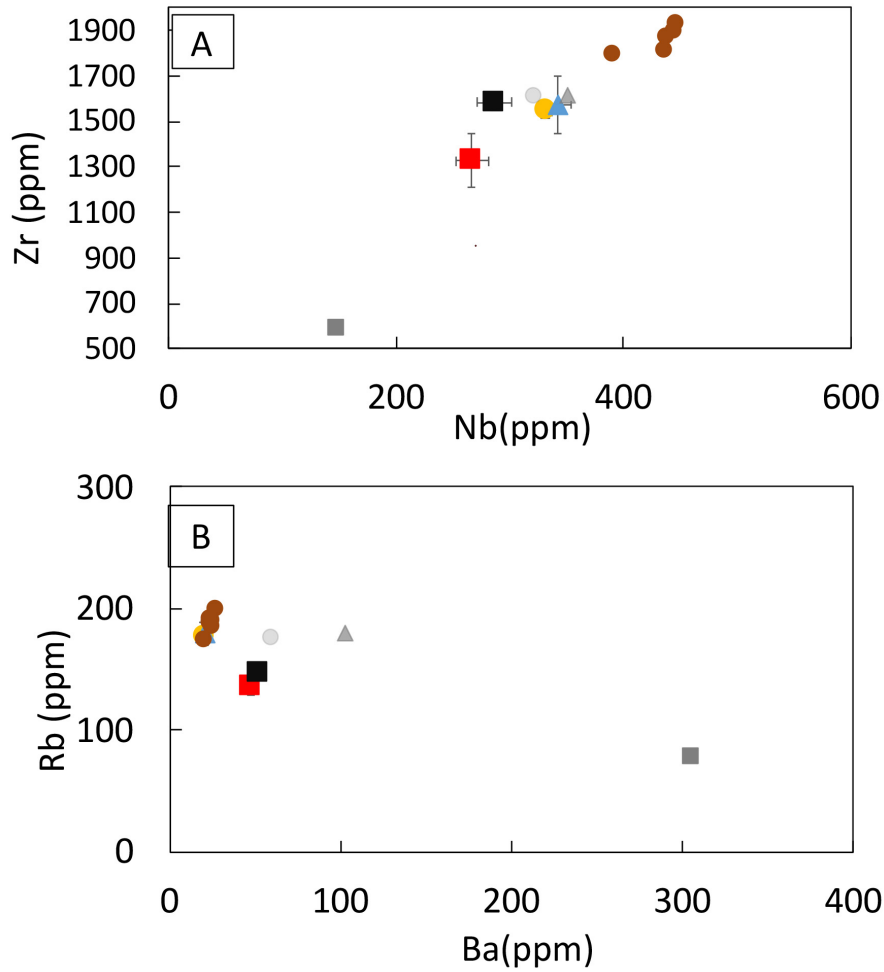


Figure 8: Trace elements binary plots: (A) Nb vs. Zr; (B) Rb vs. Ba. Legend as in Figure 7.

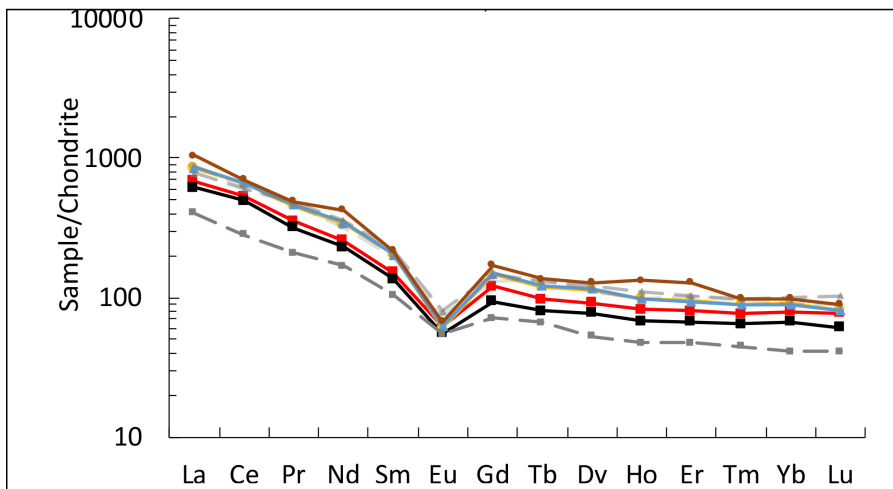


Figure 9: Rare Earth Elements distribution in the chondrite-normalized plot (C1 chondrite normalization values from McDonough & Sun, 1995). As in the major and trace elements diagrams of Figures 7 and 8, SLV and BDT samples are in almost total overlap. Legend as in Figure 7.

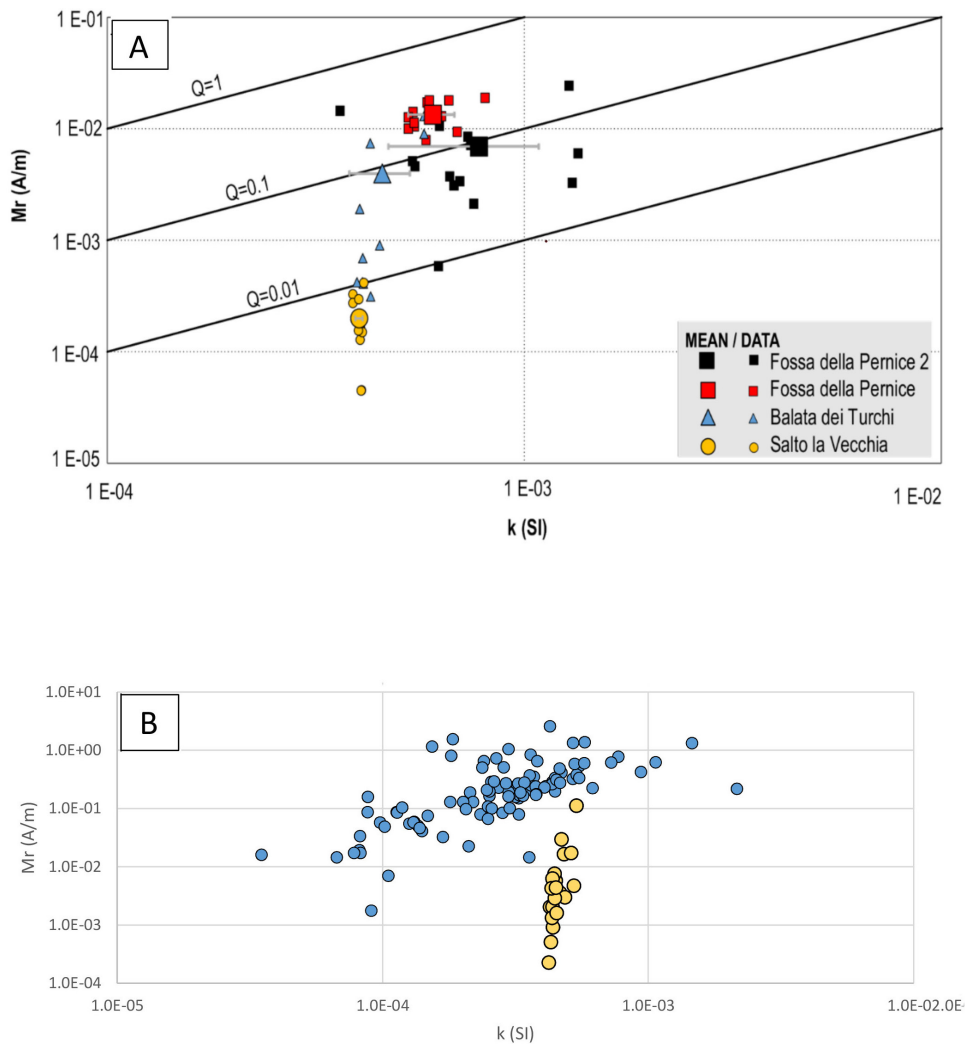


Figure 10: (A) Natural remanent magnetization intensity (M_r) vs. magnetic susceptibility (k) values for all obsidian samples from Pantelleria; sloping Q (Königsberger ratio, see text) lines are calculated for a local geomagnetic field intensity of 44,700 nT; (B) Natural remanent magnetization intensity (M_r) vs. magnetic susceptibility (k) values for archeological obsidians found at Ustica settlements. Yellow circles are obsidians compositionally peralkaline (i.e., from Pantelleria), blue circles are obsidians from Lipari (source: Foresta Martin et al., 2017). Note the striking similarity of rock magnetic parameters for the archeological obsidians of Ustica with the geological samples from Balata dei Turchi and the close vicinity with those of Salto La Vecchia.

present, respectively (Lambeck et al., 2011; Abelli et al., 2014). Therefore, Pantelleria was closer to the Sicilian coast than Lipari, given the presence of a large continental platform to the south-west of Sicily (Lodolo & Ben-Avraham, 2015).

The distribution of Pantelleria obsidians in Sicily shows a singular bipartition: while the archaeological sites of the central-western sector have variable percentages of Pantellerian obsidians, though always lower than Lipari obsidians, the sites of the eastern sector of Sicily are completely devoid. For example, a site particularly rich in Pantellerian obsidian artefacts was reported by Francaviglia and Piperno (1987) and Francaviglia (1988). These obsidians were discovered in the Neolithic settlement of Grotta dell'Uzzo, in north-western Sicily, where a significant percentage (39%) of obsidian from Pantelleria was found, compared to a relative majority of Lipari (61%). At the Grotta Maiorana at Paceco (Trapani), Pantellerian obsidian artefacts total 79% of obsidian clasts; at Casalicchio (Agrigento) Pantellerian obsidians equate to 57% (Tykot pers. communication to FFM). An overall average, from a total of 1882 obsidians analyzed by Tykot, across 28 archaeological sites in Sicily, reveal 93% are attributable to Lipari and 7% to Pantelleria (Tykot et al., 2013; Tykot, 2017a, b).

A proximity preference criterion seems to be viable to explain the movement of obsidian from the various sources. Routes from North Africa to Sicily had Pantelleria as an obvious landmass and target location for extraction of obsidian (Camps, 1974; Mulazzani et al., 2010; Abelli et al., 2014). Nevertheless, sea-routes between southern Italy and Sicily have an immediate terminus at Lipari. In this scenario, the position of Ustica is considerably closer to Lipari (~160 km) with respect to Pantelleria (~230 km). Petrographic and geochemical analyses were particularly helpful in the fine discrimination of sub-sources, however they proved to be inconclusive for ultra-fine distinctions amongst similar obsidian samples. Moreover, although only a very low quantity of material is required (less than 10 mg of glass), this is a destructive approach that sometimes cannot be applied. Obsidian hydration did not offer any particular advantage in this case study.

Paleomagnetic and magnetic susceptibility data are obtained in a fairly rapid and simple way. The longevity of the samples is not affected by analyses and the obsidian does not undergo alteration, nor is it affected thermally. Even using a limited number of samples, the *NRM* and *k* values of Pantellerian obsidians showed to be typical from one site to another. The parameter that varies mostly across the sites is *NRM*, and this likely depends on the amount of single domains of ferromagnetic minerals contained in the lavas. Previous works on Pantelleria peralkaline rhyolitic lavas (Speranza et al., 2010) and ignimbrites (Speranza, Di Chiara, & Rotolo, 2012) reveal that magnetite is the main ferromagnetic mineral of these rocks.

The comparison with archaeological obsidians from Ustica settlements (Figure 10B), shows that different obsidians may be assigned on chemical basis to Pantelleria or to Lipari. Furthermore, the different magnetic properties among Pantelleria sub-sources suggest that Balata dei Turchi is the most probable extraction site for Pantelleria obsidians found at Ustica.

9 Conclusive Remarks

Neolithic to Bronze Age obsidians of pantelleritic composition have been recovered in many archaeological settlements of the western Mediterranean. Although their provenance can be unmistakably tracked to Pantelleria, the island has at least four possible sub-sources, two of which have certainly been exploited in antiquity (Belluomini & Taddeucci, 1970; Bigazzi et al., 1971; Francaviglia, 1988).

We clarified some redundancy in proposed Pantelleria obsidian localities, showing that at least two of them cannot be clearly related to a specific outcrop (e.g. Lago di Venere, Gelkhmar), but rather to the finding of loose obsidian fragments.

With the aim to find a methodological and analytical protocol able to unravel subtle petrographic and chemical differences among similar peralkaline obsidian rocks, we applied a multi-disciplinary/multi-analytical approach (major and trace elements microanalyses, infrared spectroscopy and paleomagnetic methods) in order to discriminate between the possible geological sources of the obsidians found across a range of archaeological sites.

Petrography revealed the presence of sparse microscopic amphibole and aenigmatite microlites in obsidians from Salto La Vecchia and Balata dei Turchi sites, respectively. Furthermore, both these minerals are absent at the two Fossa della Pernice obsidian sites.

Major element geochemistry permitted the discrimination of two super-groups, Fossa della Pernice from Balata dei Turchi-Salto la Vecchia. Correspondingly, trace elements further distinguished these groups, with geochemical variation best evidenced by Rare Earth Elements. However, trace elements proved unsuccessful in distinguishing Salto La Vecchia from Balata dei Turchi obsidians, which are in chemical overlap. Additionally, FT-IR microspectroscopy did not reveal consistent differences in the glass H_2O content of the three sub-sources.

Rock magnetic methods were successful in discriminating the four Pantellerian sub-sources (FP 1, FP 2, BDT, SLV), displaying that natural remanent magnetization is a varying parameter across the three sites, ranging from 3×10^{-4} A/m (Salto La Vecchia) to 2×10^{-2} A/m (Fossa della Pernice). Thus, using magnetic remanence together with magnetic susceptibility, obsidians from the three sites could be readily distinguished.

The comparison with a set of pantelleritic (from geochemistry) archaeological obsidians from a Bronze Age settlement at Ustica indicated that these obsidians were very likely quarried from the Balata dei Turchi site at Pantelleria, which is

also the site offering the most favorable obsidian working conditions, i.e. workability, accessibility and proximity to the sea. Such conditions ensured an easy, efficient and safe transport to workshop and/or trading destinations.

Acknowledgments: Thanks are due to Erika Rodo for having provided samples BDT and for help in sample preparation for FT-IR analyses and to Nina Jordan for critical evaluation of the manuscript. We also thank Victoria Smith at the University of Oxford for allowing us analytical time on the Electron Microprobe. We also wish to thank M.S. Shackle, one anonymous reviewer and the Editor K.I. Michalak for their helpful suggestions which greatly improved the manuscript.

References

- Abelli, L., Agosto, M. V., Casalbore, D., Romagnoli, C., Bosman, A., Antonioli, F., . . . Chiocci, F. L. (2014). Marine geological and archaeological evidence of a possible pre-Neolithic site in Pantelleria Island, Central Mediterranean Sea. In Harff, J., Bailey, G., & Luth, F. (Eds.), *Geology and Archaeology: Submerged Landscapes of the Continental Shelf*. London: Geological Society of London. <https://doi.org/10.1144/SP411.6>
- Acquafredda, P., Andriani, T., Lorenzoni, S., & Zanettin, E. (1999). Chemical characterization of obsidians from different Mediterranean sources by non-destructive SEM-EDS analytical method. *Journal of Archaeological Science*, 26(3), 315–325. <https://doi.org/10.1006/jasc.1998.0372>
- Belluomini, G., & Taddeucci, A. (1970). Studi sulle ossidiane italiane I: contenuto e composizione isotopica dell' uranio e del torio. *Periodico di Mineralogia*, 39, 387–395.
- Bigazzi, G., Bonadonna, F. P., Belluomini, G., & Malpieri, L. (1971). Studi sulle ossidiane italiane IV. Datazione con il metodo delle tracce di fissione. *Bollettino della Società Geologica Italiana*, 90, 469–480.
- Camps, G. (1974). *Les Civilisations Pre-historique de l'Afrique Du Nord et du Sahara*. Paris: CNRS.
- Cattani, M., Cerasetti, B., Mascellani, M., Nicoletti, F., Orazi, R., Ramirez, J., . . . Zocchi, M. (1997). *Carta Archeologica dell'Isola di Pantelleria. Scavi e Ricerche del Dipartimento di Archeologia. Catalogo a cura di Maria Teresa Guaitoli* (pp. 93–102). Bologna, Italy: University Press.
- Crisci, G. M., Ricq-de Bouard, M., Lanzaframe U., & De Francesco, A.M. (1994). I. Nouvelle méthode d'analyse et provenance de l'ensemble des obsidiennes néolithiques du Midi de la France. *Gallia préhistoire*, 36(1), 299–309.
- Di Genova, D., Romano, C., Hess, K. U., Vona, A., Giordano, D., Dingwell, D. B., & Behrens, H. (2013). The rheology of peralkaline rhyolites from Pantelleria island. *Journal of Volcanology and Geothermal Research*, 249, 201–216. <https://doi.org/10.1016/j.jvolgeores.2012.10.017>
- Foresta Martin, F., Di Piazza, A., D'Oriano, C., Carapezza, M. L., Paonita, A., Rotolo, S. G., & Sagnotti, L. (2017). New insights on the provenance of obsidian fragments of Ustica Island (Palermo, Sicily). *Archaeometry*, 59(3), 435–454. <https://doi.org/10.1111/arcm.12270>
- Foresta Martin, F., & La Monica, M. (2019). The Black Gold that came from the sea. A review of Obsidian studies at the island of Ustica. *Annals of Geophysics*, 62(1), 14. <https://doi.org/10.4401/ag-7686>
- Foresta Martin, F., & Tykot, R. H. (2019). Characterization and Provenance of Archaeological Obsidian from Pirozza-Spalmatore, a Site of Neolithic Colonization on the Island of Ustica (Sicily). *Open Archaeology*, 5(1), 4–17. <https://doi.org/10.1515/opar-2019-0002>
- Francaviglia, V. (1984). Characterization of Mediterranean obsidian sources by classical petrochemical methods. *Preistoria Alpina- Museo Tridentino di Scienze Naturali*, 20, 311–332.
- Francaviglia, V. (1988). Ancient obsidians sources on Pantelleria (Italy) (1988). *Journal of Archaeological Science*, 15(2), 109–122. [https://doi.org/10.1016/0305-4403\(88\)90001-5](https://doi.org/10.1016/0305-4403(88)90001-5)
- Francaviglia, V., & Piperno, M. (1987). La répartition et la provenance de l'obsidienne archéologique de la Grotta dell'Uzzo et de Monte Cofano (Sicile). *ArchéoSciences, revue d'Archéométrie*, 11(1), 31-39.
- Freund, K. (2014). A Multi-Scalar Analysis of the Politics of Obsidian Consumption in the West Mediterranean (ca. 6th-2nd millennia B.C.) Ph.D Thesis, Mc. Master University. <https://macsphere.mcmaster.ca/handle/11375/16036>
- Freund, K. P., Tykot, R. H., & Vianello, A. (2015). Blade production and the consumption of obsidian in Stentinello period Neolithic Sicily. *Comptes Rendus. Palévol*, 14(3), 207–217. <https://doi.org/10.1016/j.crvp.2015.02.006>
- Freund, K. P., Tykot, R. H., & Vianello, A. (2017). Contextualizing the Role of Obsidian in Chalcolithic Sicily (c. 3500–2500 BC). *Lithic Technology*, 42(1), 35–48. <https://doi.org/10.1080/01977261.2017.1290335>
- Jochum, K. P., Stoll, B., Herwig, K., Willbold, M., Hofmann, A. W., Amini, M., . . . Raczek, I. (2006). MPI-DING reference glasses for in situ microanalysis: New reference values for element concentrations and isotope ratios. *Geochemistry Geophysics Geosystems*, 7(2), n/a. Retrieved from <https://agupubs.onlinelibrary.wiley.com/doi/full/10.1029/2005gc001060> <https://doi.org/10.1029/2005GC001060>
- Jordan, N. J., Rotolo, S. G., Williams, R., Speranza, F., McIntosh, W. C., Branney, M. J., & Scaillet, S. (2018). Explosive eruptive history of Pantelleria, Italy: Repeated caldera collapse and ignimbrite formation at a peralkaline volcano. *Journal of Volcanology and Geothermal Research*, 349, 47–73. <https://doi.org/10.1016/j.jvolgeores.2017.09.013>
- Kono, M. (2015). 5.01 - Geomagnetism: An Introduction and Overview. In G. Schubert (Ed.), *Treatise on Geophysics* (pp. 1–13). Elsevier. <https://doi.org/10.1016/B978-0-444-53802-4.00095-6>

- Lambeck, K., Antonioli, F., Anzidei, M., Ferranti, L., Leoni, G., Scicchitano, G., & Silenzi, S. (2011). Sea level change along the Italian coast during the Holocene and projections for the future. *Quaternary International*, 232(1-2), 250–257. <https://doi.org/10.1016/j.quaint.2010.04.026>
- Lanzo, G., Landi, P., & Rotolo, S. G. (2013). Volatiles in pantellerite magmas: A case study of the Green Tuff Plinian eruption (Island of Pantelleria, Italy). *Journal of Volcanology and Geothermal Research*, 262, 153–163. <https://doi.org/10.1016/j.jvolgeores.2013.06.011>
- Leighton, R. (1999). *Sicily Before History: An Archaeological Survey from the Palaeolithic to the Iron Age*. Cornell University Press.
- Lodolo, E., & Ben-Avraham, Z. (2015). A submerged monolith in the Sicilian Channel (central Mediterranean Sea): Evidence for Mesolithic human activity. *Journal of Archaeological Science: Reports*, 3, 398–407. <https://doi.org/10.1016/j.jasrep.2015.07.003>
- Macdonald, R. (1974). Nomenclature and petrochemistry of the peralkaline oversaturated extrusive rocks. In Bailey D. K., Barberi F., & Macdonald R. (Eds.), *Oversaturated peralkaline volcanic rocks*. [Special Issue]. *Bulletin of Volcanology*, 38, 498–516. <https://doi.org/10.1007/BF02596896>
- McDonough, W. F., & Sun, S. S. (1995). The composition of the Earth. *Chemical Geology*, 120(3-4), 223–253. [https://doi.org/10.1016/0009-2541\(94\)00140-4](https://doi.org/10.1016/0009-2541(94)00140-4)
- Mahood, G. A., & Hildreth, W. (1986). Geology of the peralkaline volcano at Pantelleria, Strait of Sicily. *Bulletin of Volcanology*, 48(2-3), 143–172. <https://doi.org/10.1007/BF01046548>
- Martinelli, M. C., Tykot, R. H., & Vianello, A. (2019). Lipari (Aeolian islands) obsidians in the late Neolithic. Artifact, supply and function. *Open Archaeology*, 5(1), 46–64. <https://doi.org/10.1515/opar-2019-0005>
- Mulazzani, S., Le Bourdonnec, F. X., Belhouchet, L., Poupeau, G., Zoughlami, J., Dubernet, S., . . . Khedhaier, R. (2010). Obsidian from the Epipalaeolithic and Neolithic eastern Maghreb. A view from the Hergla context (Tunisia). *Journal of Archaeological Science*, 37(10), 2529–2537. <https://doi.org/10.1016/j.jas.2010.05.013>
- Neave, D. A., Fabbro, G., Herd, R. A., Petrone, C. M., & Edmonds, M. (2012). Melting, differentiation and degassing at the Pantelleria volcano, Italy. *Journal of Petrology*, 53(3), 637–663. <https://doi.org/10.1093/petrology/egr074>
- Nicoletti, F. (1997) Il commercio preistorico dell'ossidiana nel Mediterraneo ed il ruolo di Lipari e Pantelleria nel più antico sistema di scambio. In Tusa, S. (Ed.), *Prima Sicilia: Alle origini della società siciliana : Albergo dei Poveri, Palermo, 18 ottobre-22 dicembre 1997* (pp. 258–269). Siracusa: Ediprint.
- Nicoletti, F. (2012). L'industria litica di Punta Fram: una nuova facies preistorica a Pantelleria. In Istituto italiano di preistoria e protostoria, *Atti della XLI Riunione scientifica: Dai cicli agli ecisti: società e territorio nella Sicilia preistorica e protostoria, San Cipirello (PA), 16-19 novembre 2006* (pp. 557–568). Firenze: Istituto Italiano di Preistoria e Protostoria.
- Orsi, P. (1899). Relazione in merito alla missione archeologica nell'isola di Pantelleria, anno 1894-95. *Monumenti Antichi dei Lincei*, 9.
- Rapisarda, M. (2007). L'età dell'ossidiana di Pantelleria. *Atti Della Accademia Peloritana Dei Pericolanti: Classe Di Scienze Fisiche, Matematiche e Naturali*, LXXXV, 1–21.
- Radi, G. (1973). Tracce di un insediamento neolitico sull'isola di Lampedusa. *Atti Soc. Toscana Sci. Nat. Mem., Serie A*, 79, 197–205.
- Scaillet, S., Rotolo, S. G., La Felice, S., & Vita-Scaillet, G. (2011). High-resolution $^{40}\text{Ar}/^{39}\text{Ar}$ chronostratigraphy of the post-caldera (<20 ka) volcanic activity at Pantelleria, Sicily Strait. *Earth and Planetary Science Letters*, 309(3-4), 280–290. <https://doi.org/10.1016/j.epsl.2011.07.009>
- Scaillet, S., Vita-Scaillet, G., & Rotolo, S. G. (2013). Millennial-scale phase relationships between ice-core and Mediterranean marine records: insights from high-precision $^{40}\text{Ar}/^{39}\text{Ar}$ dating of the Green Tuff of Pantelleria, Sicily Strait. *Quaternary Science Reviews*, 78, 141–154. <https://doi.org/10.1016/j.quascirev.2013.08.008>
- Speranza, F., Landi, P., D'Ajello Caracciolo, F., & Pignatelli, A. (2010). Paleomagnetic dating of the most recent silicic eruptive activity at Pantelleria (Strait of Sicily). *Bulletin of Volcanology*, 72(7), 847–858. <https://doi.org/10.1007/s00445-010-0368-5>
- Speranza, F., Di Chiara, A., & Rotolo, S. G. (2012). Correlation of welded ignimbrites on Pantelleria (Strait of Sicily) using paleomagnetism. *Bulletin of Volcanology*, 74(2), 341–357. <https://doi.org/10.1007/s00445-011-0521-9>
- Stevenson, C. M., & Novak, S. W. (2011). Obsidian hydration dating by infrared spectroscopy: method and calibration. *Journal of Archaeological Science*, 38(7), 1711–1726. <https://doi.org/10.1016/j.jas.2011.03.003>
- Tozzi, C. (1968). Relazione preliminare sulla I e II campagna di scavi effettuati a Pantelleria. *Rivista di scienze preistoriche*, 23(2), 315–388.
- Trump, D. H. (1966). Skorba. Excavations carried out on behalf of the National Museum of Malta, 1961–1963 (Reports of the Research Committee of the Society of Antiquaries of London, Vol. XXII). London: Society of Antiquaries of London.
- Tufano, E., D'Amora, A., Trifuoggi, M., & Tusa, S. (2012). L'ossidiana di Pantelleria: studio di caratterizzazione e provenienza alla luce della scoperta di nuovi giacimenti. In *Atti della XLI Riunione scientifica: Dai cicli agli ecisti : società e territorio nella Sicilia preistorica e protostoria, San Cipirello (PA), 16-19 novembre 2006* (pp. 839–849). Firenze: Istituto Italiano di Preistoria e Protostoria.
- Tusa, S. (1997). *Prima Sicilia: Alle origini della società siciliana : Albergo dei Poveri, Palermo, 18 ottobre-22 dicembre 1997*. Siracusa: Ediprint.
- Tusa, S. (2016). Il popolamento di Pantelleria e Lampedusa dalle prime frequentazioni neolitiche al villaggio di Mursia. *Scienze dell'Antichità*, 22(2), 363–385.
- Tykot, R. H. (1996). Obsidian procurement and distribution in the central and western Mediterranean. *Journal of Mediterranean Archaeology*, 9(1), 39–82. <https://doi.org/10.1558/jmea.v9i1.39>
- Tykot, R. H. (2017a). A decade of portable (hand-held) X-ray fluorescence spectrometer analysis of obsidian in the Mediterranean: Many advantages and few limitations. *MRS Advances*, 2(33-34), 1769–1784. <https://doi.org/10.1557/adv.2017.148>
- Tykot, R. H. (2017b). Obsidian Studies in the Prehistoric Central Mediterranean: After 50 Years, What Have We Learned and What Still Needs to Be Done? *Open Archaeology*, 3(1), 264–278. <https://doi.org/10.1515/opar-2017-0018>

- Tykot, R. H. (2019). Geological sources of obsidian on Lipari an artifact production and distribution in the Neolithic to Bronze Age Central Mediterranean. *Open Archaeology*, 5(1), 83–105. <https://doi.org/10.1515/opar-2019-0007>
- Tykot, R. H., Freund, K. P., & Vianello, A. (2013). Source Analysis of Prehistoric Obsidian Artifacts in Sicily (Italy) using pXRF. In R. A. Armitage & J. H. Burton (Eds.), *Archaeological Chemistry VIII*. (ACS Symposium Series, Vol. 1147, pp. 195–210). American Chemical Society. <https://doi.org/10.1021/bk-2013-1147.ch011>
- Tykot, R. H., & Foresta Martin, F. (2020). Analysis by pXRF of Prehistoric Obsidian Artifacts From Several Sites on Ustica (Italy): Long-Distance Open-Water Distribution From Multiple Island Sources During the Neolithic and Bronze Ages. *Open Archaeology*, 6(1), 348–392. <https://doi.org/10.1515/opar-2020-0118>
- Vargo, B. (2003). *Characterization of obsidian sources in Pantelleria, Italy*. (Master's thesis). University of South Florida retrieved from <https://digital.lib.usf.edu/SFS0024913/00001>
- White, J. C., Parker, D. F., & Ren, M. (2009). The origin of trachyte and pantellerite from Pantelleria, Italy: Insights from major elements, trace elements, and thermodynamic modelling. *Journal of Volcanology and Geothermal Research*, 179(1-2), 33–55. <https://doi.org/10.1016/j.jvolgeores.2008.10.007>
- Williams-Thorpe, O. (1995). Obsidian in the Mediterranean and the Near East: A provenancing success story. *Archaeometry*, 37(2), 217–248. <https://doi.org/10.1111/j.1475-4754.1995.tb00740.x>
- Zilhão, J. (2014). Early prehistoric navigation in the Western Mediterranean: Implications for the Neolithic transition in Iberia and the Maghreb. *Eurasian Prehistory*, 11, 185–200